EE4-55
EE9AO11

IMPERIAL COLLEGE LONDON

DEPARTMENT OF ELECTRICAL AND ELECTRONIC ENGINEERING
EXAMINATIONS 2011

MSc and EEE PART IV: MEng and ACGI

Corrected Copy

MEMS AND NANOTECHNOLOGY

Monday, 23 May 10:00 am

Time allowed: 3:00 hours

There are FIVE questions on this paper.

Answer Question 1.
Answer Question 2 OR Question 3.
Answer Question 4 OR Question 5.

Question 1 carries 40% of the marks. Remaining questions carry 30% each.

Any special instructions for invigilators and information for candidates are on page 1.

Examiners responsible First Marker(s) : Z. Durrani, A.S. Holmes, Z. Durrani
Second Marker(s) : A.S. Holmes, Z. Durrani, A.S. Holmes

© Imperial College London

Information for Candidates

The following physical constants may be used:

electron charge:	$e = 1.6 \times 10^{-19}$ C
electron mass:	$m_e = 9.1 \times 10^{-31}$ kg
Planck's constant:	$h = 6.63 \times 10^{-34}$ J s
Boltzmann's constant:	$k_B = 1.38 \times 10^{-23}$ J/K

The piezoresistive equations for silicon, referred to axes aligned to the <100> directions, are:

$$E_1 / \rho_e = J_1[1 + \pi_{11}\sigma_1 + \pi_{12}(\sigma_2 + \sigma_3)] + J_2\pi_{44}\tau_{12} + J_3\pi_{44}\tau_{13}$$
$$E_2 / \rho_e = J_2[1 + \pi_{11}\sigma_2 + \pi_{12}(\sigma_1 + \sigma_3)] + J_1\pi_{44}\tau_{12} + J_3\pi_{44}\tau_{23}$$
$$E_3 / \rho_e = J_3[1 + \pi_{11}\sigma_3 + \pi_{12}(\sigma_1 + \sigma_2)] + J_1\pi_{44}\tau_{13} + J_2\pi_{44}\tau_{23}$$

The maximum stress σ_{max} in a square membrane of side L and thickness h subject to a uniformly distributed load p is:

$$\sigma_{max} \approx 0.3\frac{pL^2}{h^2}$$

 Copyright Imperial College London

This question is compulsory

1. a) In a one-dimensional semiconductor quantum well of width L= 5 nm, the energy levels may be approximated by:

$$E_n = \frac{n^2 \pi^2 \hbar^2}{2mL^2}$$

where the reduced Plank's constant $\hbar$ = 1.055 × 10^{-34} J.s and the electron effective mass m = 3 × 10^{-31} kg. At temperature T = 300 K, if there is a 1% probability that energy level E_1 is occupied by an electron, what is the probability that level E_2 is occupied? [5]

b) Figure 1.1 shows a double potential well, where two potential wells of width L are separated by a potential barrier of width D and height V_1. Here, the energy within the wells is zero and D is narrow enough such that the wavefunctions overlap. (i) Write down the wavevectors k_I, k_{II}, and k_{III}, for the wavefunctions in regions I, II and III respectively. (ii) Sketch, without solving Schrödinger's equation, the wavefunctions corresponding to the first two energy levels E_1 and E_2. Justify, briefly, your argument for the shape of the wavefunctions. [5]

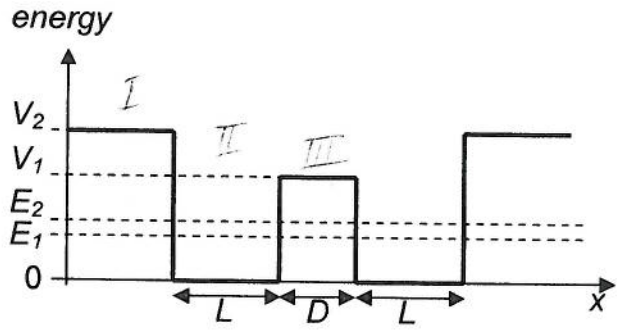

Figure 1.1

c) Using suitable diagrams, show the fabrication process flow for a CMOS inverter. [5]

Question 1 continues on the next page

 Copyright Imperial College London

Question 1 continued

d) Figure 1.2 shows the lattice of graphene, with translational vectors a_1 and a_2. For three carbon nanotubes, with Chiral vector C_h corresponding to the vectors A, B and C (Figure 1.2), write down the translational numbers (n,m). Hence, determine if the nanotubes are metallic or semiconducting. [5]

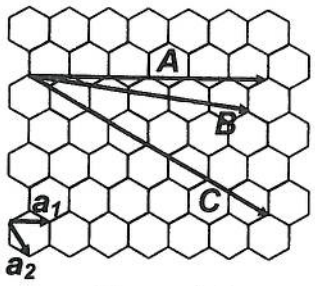

Figure 1.2

e) Show from the geometry of the unit cell that the sidewalls of an anisotropically etched cavity in a (100)-oriented silicon wafer are expected to form an angle of 54.7° with the wafer surface. Show also that vertical sidewalls can be obtained by anisotropically etching a (110)-oriented silicon wafer. What is the limiting shape of the opening at the wafer surface for each of these wafer orientations? [5]

f) An electron beam lithography system has an acceleration voltage of 100 kV and a beam convergence angle of 1 milliradian. Estimate the resolution achievable with this system if it is limited only by diffraction. In practice what other factors will limit the minimum achievable feature size in a resist layer? [5]

g) Briefly explain the operational principles of material bimorph and shape bimorph electrothermal actuators and sketch typical geometries for such devices. Also highlight the differences between these two actuator types in terms of functionality and ease of fabrication. [5]

h) Starting from the elementary bending equation, derive an expression for the transverse stiffness of a simple cantilever in terms of its dimensions and Young's modulus. Also derive an expression for the maximum tensile strain, and hence obtain an expression for the maximum strain in terms of the end deflection and the beam dimensions. [5]

 Copyright Imperial College London

2. a) The $|1s\rangle$ state of the hydrogenic atom can be written as $\psi_{100} = A\exp(-Zr/a_0)$, in spherical coordinates (r, θ, φ). Here, Z is the atomic number and a_0 is the Bohr radius. Find the normalisation constant A. [10]

b) Figure 2.1 shows a Si atom, labelled '1', within the Si unit cell. The bonds b_1, b_2, b_3 and b_4 connect this atom to its nearest neighbour atoms. (i) What is the bond length? (ii) Write down, in the form $[uvw]$, the fundamental direction vectors parallel to these bonds. Assume that the bonds point from atom 1 towards the nearest neighbour atoms. [5]

c) By approximating a Si atom within the crystal as a hydrogenic atom, construct the hybridised wavefunctions $|2p_x\rangle$, $|2p_y\rangle$ and $|2p_z\rangle$. Sketch these wavefunctions, and the $|2s\rangle$ wavefunction. You may use the $|2s\rangle$ and $|2p\rangle$ states of the hydrogenic atom, in spherical coordinates (r, θ, φ), given below:

$$|2s\rangle = \psi_{200} \sim \left(1 - \frac{Zr}{2a_0}\right) e^{\frac{-Zr}{2a_0}}$$

$$|2p_0\rangle = \psi_{210} \sim e^{\frac{-Zr}{2a_0}} r\cos\theta$$

$$|2p_{\pm 1}\rangle = \psi_{21,\pm 1} \sim e^{\frac{-Zr}{2a_0}} e^{\pm i\phi} r\sin\theta$$ [8]

d) Hence, construct the $|sp^3\rangle$ wavefunction pointing along the direction parallel to bond b_3 (Figure 2.1). Sketch this wavefunction. [7]

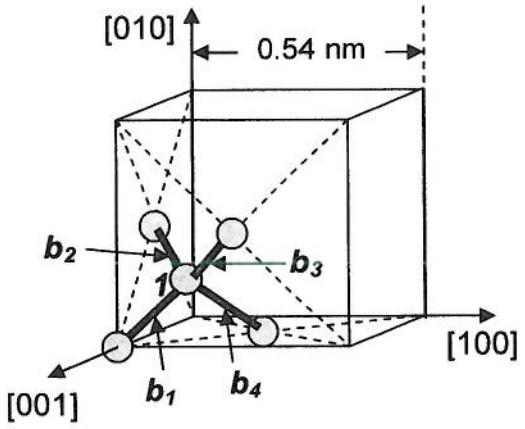

Figure 2.1

3. Figure 3.1 shows an n-channel, depletion mode Si MOSFET, where the channel is formed by a Si layer of thickness D, lying on a SiO_2 substrate. The Si channel doping concentration is N_D. A top SiO_2 layer of thickness t_{ox} forms the gate oxide.

a) Assuming 'flat-band' conditions at gate voltage $V_g = 0$ V and $V_{ds} = 0$ V, sketch the energy bands along the line AA' for carrier depletion in the n-channel. Your diagram should show the conduction and valance band edges E_c and E_v , and the intrinsic level E_i, in the Si. The diagram should also show the Fermi energy E_F, and the width of the depletion region W_D. [5]

b) Sketch the charge per unit volume $\rho(x)$ along the line AA'. [5]

c) Hence, by solving Poisson's equation, $-\frac{\partial^2 V}{\partial x^2} = \frac{\partial F}{\partial x} = \frac{\rho(x)}{\varepsilon_0 \varepsilon_{Si}}$ in the Si, find the potential V_s at the Si – gate oxide interface, at $x = 0$. Here, ε_0 is the permittivity of free space, ε_{Si} is the relative permittivity of Si, F is the electric field and V is the potential. [15]

d) Using the result of part (c), write down an expression for the threshold voltage V_{th}, in terms of the Si layer thickness D. [5]

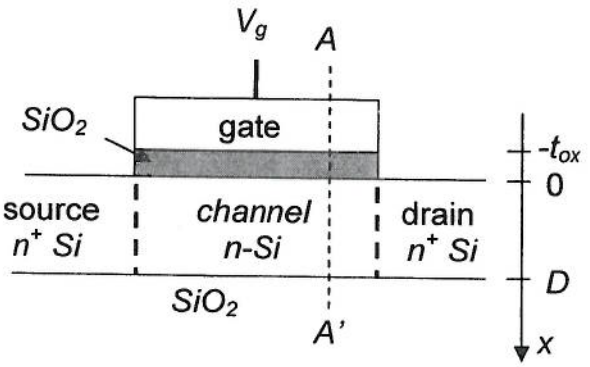

Figure 3.1

 Copyright Imperial College London

4. a) List the four main transductions mechanisms used in MEMS sensors, and briefly describe their underlying principles. Which two mechanisms are most widely used, and why? [8]

b) Figure 4.1 shows the schematic of a membrane pressure sensor with piezoresistive readout. The device is fabricated in a (100)-oriented wafer, and the membrane edges are aligned to <110> directions. Readout is via a single p-type piezoresistor positioned at the mid-point of one edge, and aligned along a <100> direction. A current is passed through the piezoresistor in the longitudinal direction, by applying a voltage V_{BA} between terminals A and B, and the resulting transverse voltage V_{CD} between C and D is taken as a measure of the membrane stress.

Starting from the piezoresistive equations for silicon, and neglecting the effect of membrane stress on the longitudinal resistance of the piezoresistor, show that the voltage V_{CD} is expected to be:

$$V_{CD} = \pi_{44}\tau_{12}\left(\frac{w}{l}\right)V_{BA}$$

where w and l are the width and length of the piezoresistor respectively. [8]

Also, by considering the equilibrium of a small triangular element, or otherwise, derive an expression for the shear stress τ_{12} in terms of the axial stresses σ_x and σ_y in the region of the piezoresistor. [6]

Hence estimate the sensor output voltage at a differential pressure of 1 kPa, assuming V_{AB} = 5 V and w/l = 0.2, if the membrane is 1000 x 1000 μm^2 in area and has a thickness of 20 μm. You may assume π_{44} = 138.1 x 10^{-11} Pa^{-1} for p-type silicon. Poisson's ratio for the relevant directions is ν = 0.064. [8]

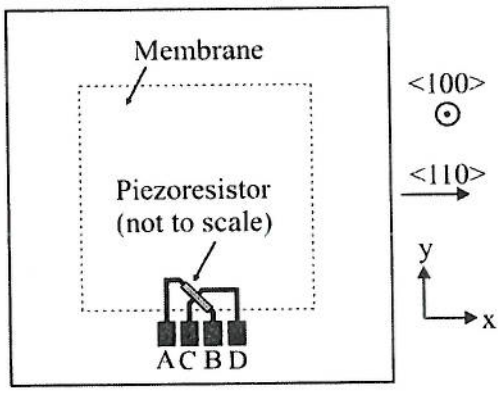

Figure 4.1

5. a) Figure 5.1 shows a flexure of length L, subject to both a transverse end load P and an axial load F. Write down the bending equation for this situation and show that it can be expressed in the form:

$$\frac{d^2v}{dx^2} - \kappa^2 v = \frac{C - Px}{EI}$$

where $v(x)$ is the deflection profile, E and I have their usual meanings, and $\kappa = \sqrt{\frac{F}{EI}}$. [6]

By solving the bending equation subject to appropriate boundary conditions, show that the transverse stiffness $k = P/v(L)$ is given by:

$$k = \frac{F}{L} \cdot \frac{\kappa L \sinh(\kappa L)}{2[1 - \cosh(\kappa L)] + \kappa L \sinh(\kappa L)}$$

Also show that, when the axial load is small, the stiffness may be written approximately as:

$$k \approx \frac{12EI}{L^3}\left[1 + \frac{FL^2}{10EI}\right]$$ [14]

b) Figure 5.2 shows the layout of a micromechanical resonator which is fabricated in a nickel mechanical layer on a silicon substrate. The mass has an area of 200 x 200 μm^2, and is supported by a hammock suspension comprising four flexures, each flexure being 100 μm long and 5 μm wide. The in-plane motion is driven and sensed via electrode arrays (not shown).

Estimate the temperature coefficient (fractional change per °C) of the resonant frequency assuming this is dominated by differential thermal expansion between the nickel layer and the substrate. Assume values of 2.5×10^{-6} K^{-1} and 13.3×10^{-6} K^{-1} for the thermal expansion coefficients of silicon and nickel respectively. [10]

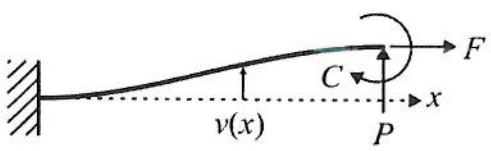

Figure 5.1

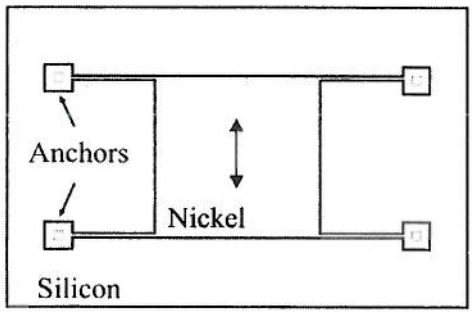

Figure 5.2

 Copyright Imperial College London

Answer, Question 1

a) The energy levels E_n in a 1-D quantum well of width L, measured from the bottom of the well E_w, are given by $E_n = \dfrac{n^2\pi^2\hbar^2}{2mL^2}$ where $n \geq 1$. These levels are shown in Fig. A1.1 below:

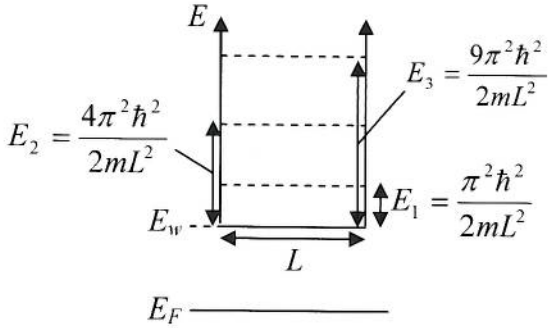

Figure A1.1

As the probability that level E_1 is occupied is 1%, this implies that the Fermi energy E_F lies below E_1 (Fig. A1.1). Using the Fermi-Dirac distribution:

$$f(E_1 + E_w) = \frac{1}{1+\exp\left(\dfrac{E_1 + E_w - E_F}{k_B T}\right)} = 0.01$$

$$\Rightarrow 1+\exp\left(\frac{E_1 + E_w - E_F}{k_B T}\right) = 100$$

$$\Rightarrow \exp\left(\frac{E_1 + E_w - E_F}{k_B T}\right) = 99$$

$$\Rightarrow E_1 + E_w - E_F = k_B T \ln 99$$

$$\Rightarrow E_1 + E_w - E_F = 0.0258 \times 4.59 = 0.12eV$$

Furthermore, $E_1 = \dfrac{\pi^2\hbar^2}{2mL^2} = \dfrac{\pi^2\left(1.055\times10^{-34}\right)^2}{2\left(3\times10^{-31}\right)\left(5\times10^{-9}\right)^2} = 0.045eV$

$$E_2 = 4E_1 = 0.18eV$$

$\therefore E_w - E_F = (E_1 + E_w - E_F) - E_w = 0.12 - 0.045 = 0.075\text{eV}$

$$\therefore f(E_2 + E_w) = \frac{1}{1+\exp\left(\dfrac{E_2 + E_w - E_F}{k_B T}\right)} = \frac{1}{1+\exp\left(\dfrac{0.18+0.075}{0.0258}\right)} = 5.1\times10^{-5} = 0.005\%$$

[5]

b) (i) The wavevectors in regions I, II, and III are as follows:

$$k_I = \sqrt{\frac{2m}{\hbar^2}(E - V_2)} \ , \ k_{II} = \sqrt{\frac{2m}{\hbar^2}E} \ , \ k_{III} = \sqrt{\frac{2m}{\hbar^2}(E - V_1)}$$

[3]

(ii) Figure A1.2a shows the ground state $\psi_{1,sngl}$ in a single quantum well of width L, where a central 'cos(kx)' section matches to exponential tails within the barriers on either side. In a double quantum well (Fig. 1.2b and Fig. 1.2c), if the ground states in the two wells overlap, then two possibilities exist, both of which satisfy the wavefunction matching conditions $\psi_1 = \psi_2$ and $\psi_1' = \psi_2'$ at a potential boundary. These give the symmetric wavefunction ψ_1 (Fig. A1.2b), and the antisymmetric wavefunction ψ_2 (Fig. A1.2c). If the central potential barrier width D tends to zero, then ψ_1 tends to the ground state of a single potential well of width $2L$ (the 'peaks' of ψ_1 move together) and ψ_2 tends to the first excited state of a single potential well of width $2L$ (the 'zero' remains at the centre of the new potential well). Therefore, ψ_1 is the ground state of the double potential well, with energy E_1, and ψ_2 is associated with the first excited state of the double potential well, with energy E_2.

Fig. A1.2a

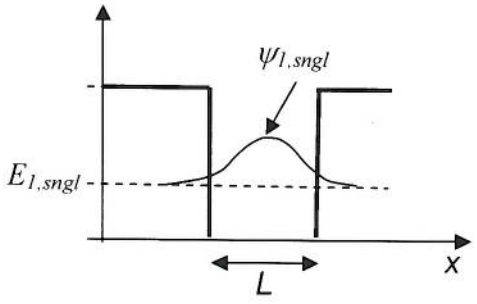

Fig. A1.2b

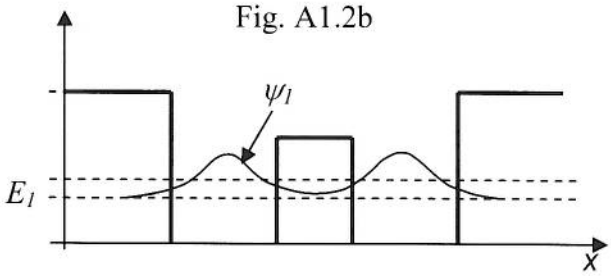

Fig. A1.2c

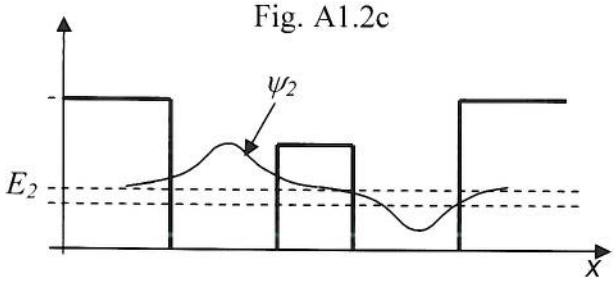

[2]

c) The fabrication process flow for a CMOS inverter is shown diagrammatically below:

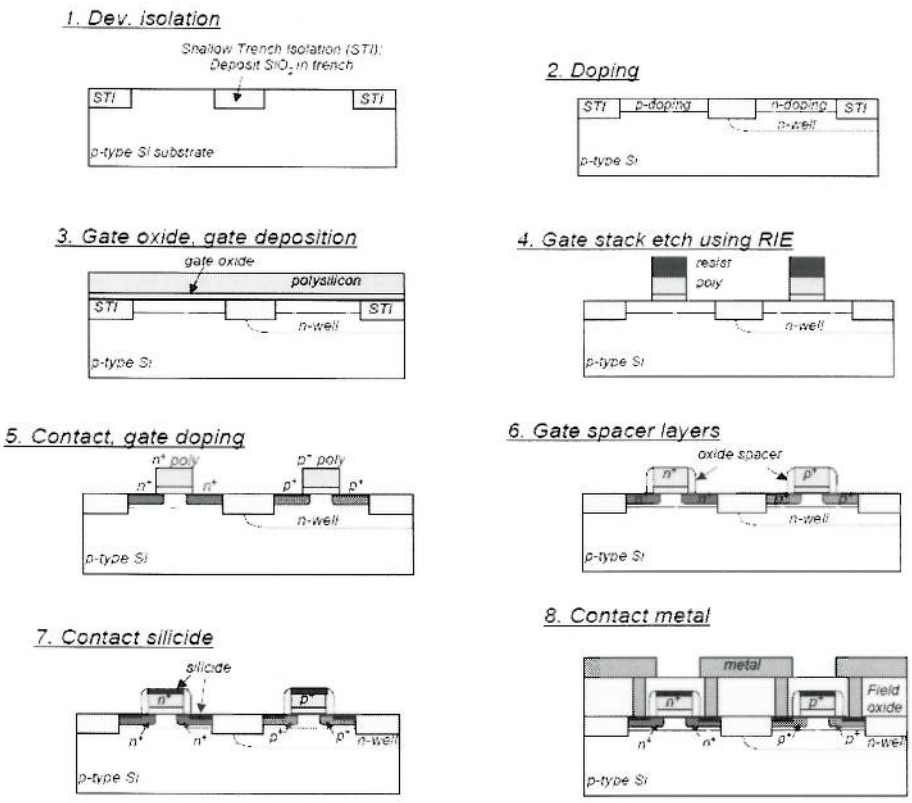

[5]

d) By inspection of Fig. 1.2, the translational numbers (n,m) of nanotubes formed when Chiral vector C_h lies along vectors A, B and C are as follows:

Along A: $(n,m) = (6, 0)$
Along B: $(n,m) = (5, 1)$
Along C: $(n,m) = (4, 4)$

[3]

A nanotube is metallic if $n = m$. If $n - m = 3j$, where j is an integer, then the nanotube is semiconducting with a small bandgap. This nanotube may behave as a metal at room temperature. If $n - m = 3j + 1$, where j is an integer, then the nanotube is a wide bandgap semiconductor.

Therefore:
(i) Nanotube 'A': $n = m$ and the tube is metallic
(ii) Nanotube 'B': $n - m = 5 - 1 = 4 = 3j + 1$ with $j = 1$. The tube is a wide bandgap semiconductor.
(iii) Nanotube 'C': $n - m = 6 - 0 = 6 = 3j$ with $j = 2$. The tube is a narrow bandgap semiconductor.

[2]

e) The sidewalls of an aniostropically etched cavity will be {111} planes, while the wafer surface is the (100) plane. The angle between any two planes is $\theta = \cos^{-1}(\mathbf{n1}\cdot\mathbf{n2})$ where **n1** and **n2** are the unit normals. For the planes in question we have $\mathbf{n1} = (\pm1,\pm1,\pm1)/\sqrt{3}$ and **n2** = (1,0,0), so $\theta = \cos^{-1}(\pm1/\sqrt{3}) = 54.7°$ or 125.3°. Only the acute angle will ever arise because the corresponding planes will be exposed first and will terminate the etch process.

Some {111} group planes are normal to the (110) plane, for example $(1\,\bar{1}\,1)$ and $(\bar{1}\,11)$, and it follows that vertical sidewalls can be obtained with a (110) wafer.

The limiting shapes are a rectangle for (100) and a parallelogram for (110). [5]

f) If the resolution is limited by diffraction, then it will be given by $R \sim \lambda/NA$ where λ is the wavelength and NA is the numerical aperture. For an electron beam system λ is the de Broglie wavelength, and NA is half the convergence angle of the beam. So:

$\lambda = h/p = h/\sqrt{(2mE)} = 6.63\text{e-}34/\sqrt{(2 \times 9.1\text{e-}31 \times 1\text{e}5 \times 1.6\text{e-}19)} = 3.89$ pm
$NA = 5\times10^{-4}$
$\Rightarrow R \sim 8$ nm

In practice, the minimum achievable feature size in resist will be larger than this because of machine-related imperfections affecting the minimum spot size (finite source size and aberrations in the electron optics) and scattering in the resist and substrate. [5]

g) Electrothermal actuators use differential thermal expansion between different parts of a structure to generate motion. In a material bimorph actuator, the differential thermal expansion occurs between two dissimilar materials that are in intimate contact, while in a shape bimorph actuator the device geometry leads to temperature differentials between different parts of a single mechanical layer. Heating is generally achieved by passing a current through either the mechanical layer or a deposited heater layer.

Material bimorph:

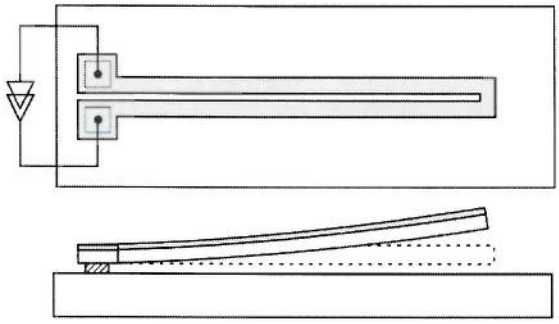

Shape bimorph:

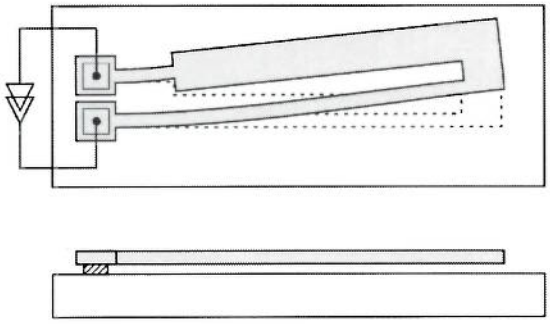

5

Material bimorph actuators generally produce out-of-plane motion, while shape bimorph generally produce in-plane motion. Shape bimorph actuators are easier to fabricate because they can be realised in a single layer. They are also less prone to unwanted deflections due to intrinsic stress and ambient temperature variations. [5]

h) The bending equation for a cantilever with a transverse end load P is:

$$M = EI\frac{d^2v}{dx^2} = P(L-x)$$

where $v(x)$ is the deflection profile, x is distance along the cantilever measured from the root, L is the cantilever length, E is Young's modulus and I is the second moment of area. Assuming a rectangular cross-section, $I = wh^3/12$ where w and h are the cross-sectional dimensions, with h being in the direction of the load P.

Integrating twice, and applying the boundary conditions $v = 0$, $v' = 0$ at $x = 0$, the deflection profile is obtained as $v(x) = (PL^3/6\text{EI})\cdot(3u^2 - u^3)$ where $u = x/L$.

Putting $u = 1$, the end deflection is $v_L = v(L) = PL^3/3EI$, so the stiffness is:

$$k = P/v(L) = 3\text{EI}/\text{L}^3$$

The axial strain varies as:

$$\varepsilon = -\frac{y}{R} \approx -y\frac{d^2v}{dx^2} = -\frac{yP(L-x)}{EI}$$

where y is the distance from the neutral axis in the direction of the applied load. The maximum tensile strain occurs when $y = -h/2$ and $x = 0$, and is given by $\varepsilon_{max} = PLh/2EI$. Combining this with the earlier result for the end deflection gives:

$$\varepsilon_{\max} = \frac{3v_L h}{2L^2}$$ [5]

Answer, Question 2

Question 2(a)

$$\psi_{100} = A\exp\left(-\frac{Zr}{a_0}\right)$$

Normalising in spherical coordinates:

$$\int_{r=0}^{\infty}\int_{\theta=0}^{\pi}\int_{\phi=0}^{2\pi}\psi_{100}^2\, r^2 \sin\theta\, dr\, d\theta\, d\phi = 1$$

$$\Rightarrow A^2\int_0^{\infty}\int_0^{\pi}\int_0^{2\pi} e^{-\frac{2Zr}{a_0}} r^2\sin\theta\, dr\, d\theta\, d\phi$$

$$= A^2\int_0^{\infty} e^{-\frac{2Zr}{a_0}} r^2\, dr \int_0^{\pi}\sin\theta\, d\theta \int_0^{2\pi} d\phi$$

$$= A^2\left|-\cos\theta\right|_0^{\pi}\cdot\left|\phi\right|_0^{2\pi}\cdot\left(\left|\frac{r^2 e^{-2Zr/a_0}}{-\frac{2Z}{a_0}}\right|_0^{\infty} - \int_0^{\infty}\frac{2r\, e^{-\frac{2Zr}{a_0}}}{-\frac{2Z}{a_0}}dr\right)$$

$$= -A^2(-1-1)\cdot(2\pi-0)\cdot\left(+\frac{2a_0}{2Z}\int_0^{\infty} r\, e^{-\frac{2Zr}{a_0}}dr\right)$$

$$= +8\pi A^2\left(\frac{a_0}{2Z}\left(\left|\frac{r\, e^{-2Zr/a_0}}{-\frac{2Z}{a_0}}\right|_0^{\infty} - \int_0^{\infty}\frac{e^{-2Zr/a_0}}{-2Z/a_0}dr\right)\right)$$

$$= +8\pi A^2\left(\frac{a_0}{2Z}\left(+\frac{a_0}{2Z}\left|\frac{e^{-\frac{2Zr}{a_0}}}{-\frac{2Z}{a_0}}\right|_0^{\infty}\right)\right)$$

$$= +8\pi A^2\left(\frac{a_0}{2Z}\right)^2\cdot\left(-\frac{a_0}{2Z}(0-1)\right)$$

$$= +8\pi A^2\left(\frac{a_0}{2Z}\right)^3 = 1$$

$$\Rightarrow \quad A = \sqrt{\frac{1}{\pi}}\left(\frac{Z}{a_0}\right)^{3/2}$$

[Marks: 10]

Question 2(b)

Looking from the top, i.e [010] direction, and from the front, i.e. [001] direction, the atoms are arranged as follows:

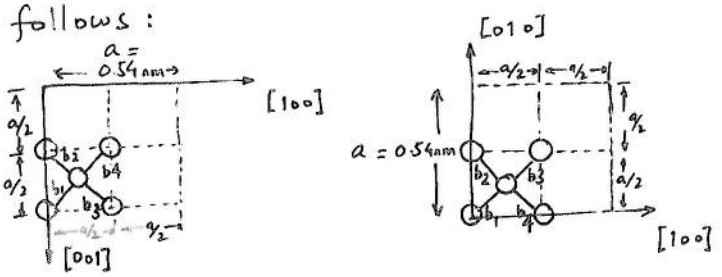

top view front view

(i) Bond Lengths are the same and are given by:

$$|b| = \sqrt{\left(\frac{a}{4}\right)^2 + \left(\frac{a}{4}\right)^2 + \left(\frac{a}{4}\right)^2} = \sqrt{3\left(\frac{a}{4}\right)^2}$$

$$= \frac{\sqrt{3}}{4}a = 0.43 \times 0.54 = 0.23 \text{ nm}$$

[1]

(ii) The fundamental direction vectors, parallel to the bonds, can be written down by inspection:

Bond 'b_1': $[\bar{1}\,\bar{1}\,1]$

Bond 'b_2': $[\bar{1}\,1\,\bar{1}]$

Bond 'b_3': $[1\,1\,1]$

Bond 'b_4': $[1\,\bar{1}\,\bar{1}]$

[4]

[Marks: 5]

Question 2(c)

$$|2S\rangle = \psi_{200} \sim \left(1 - \frac{Zr}{2a_0}\right) e^{-Zr/2a_0}$$

$$|2P_0\rangle = \psi_{210} \sim e^{-Zr/2a_0} \cdot r\cos\theta$$

$$|2P_{\pm1}\rangle = \psi_{21,\pm1} \sim e^{-Zr/2a_0} \cdot e^{\pm i\phi} r\sin\theta$$

The $|2p\rangle$ states can be rewritten as (see diagram):

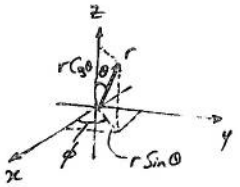

$$|2P_z\rangle = \psi_{210} \sim r\cos\theta\, e^{-Zr/2a_0}$$

$$= z\, e^{-Zr/2a_0}$$

(z: axis)

and

$$|2P_{\pm1}\rangle = \psi_{21,\pm1} = e^{-Zr/2a_0} e^{\pm i\phi} r\sin\theta$$

$$= e^{-Zr/2a_0}(r\sin\theta)(\cos\phi \pm i\sin\phi)$$

$$= e^{-Zr/2a_0}(x \pm iy)$$

We may then construct the linear combinations:

$$|2P_x\rangle = \frac{\psi_{21,1} + \psi_{21,-1}}{2} = x e^{-Zr/2a_0}$$

$$|2P_y\rangle = \frac{\psi_{21,1} - \psi_{21,-1}}{2i} = y e^{-Zr/2a_0}$$

These states are sketched below:

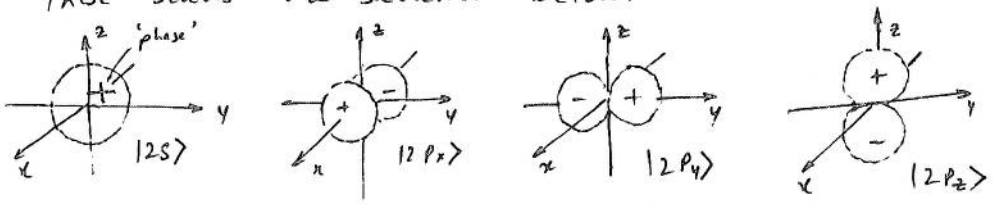

[Marks: 8]

Question 2 (d)

The bond 'b_3' points along the [111] fundamental direction. We may construct further linear combinations, using the $|2s\rangle$, $|2p_x\rangle$, $|2p_y\rangle$ and $|2p_z\rangle$ states:

First combination:

$$|x+y+z\rangle = |2p_x\rangle + |2p_y\rangle + |2p_z\rangle$$
$$= (x+y+z)\, e^{-Zr/2a_0}$$

This is aligned along the [111] direction

We then construct the combination:

$$|sp^3\rangle = |2s\rangle + |x+y+z\rangle$$
$$= \left(1 - \frac{Zr}{2a_0}\right) e^{-Zr/2a_0} + (x+y+z)\, e^{-Zr/2a_0}$$

This points along the [111] direction

The wavefunction is plotted below:

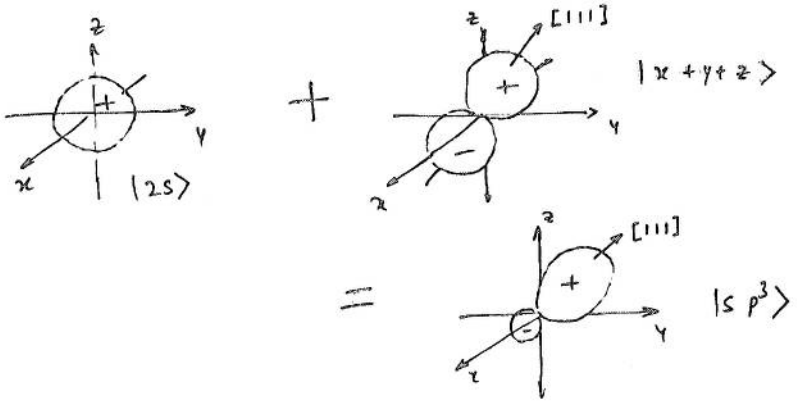

[Marks: 7]

Answer, Question 3

(a) The energy band diagrams along the line *AA'* are shown in Fig. A3.1 below. The 'flat-band' condition is also shown for completeness (this is not asked in the question):

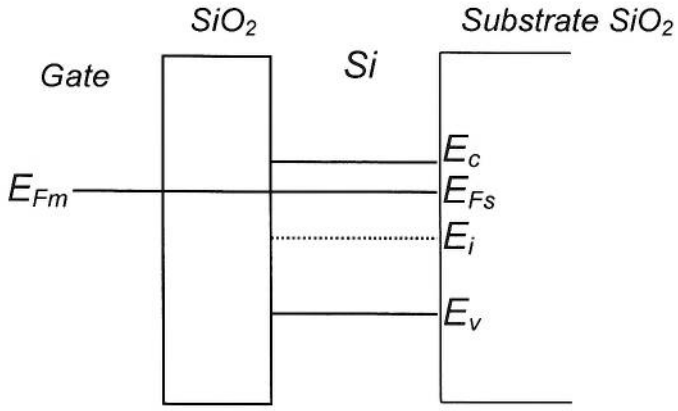

Fig. A3.1a. 'Flat-band'

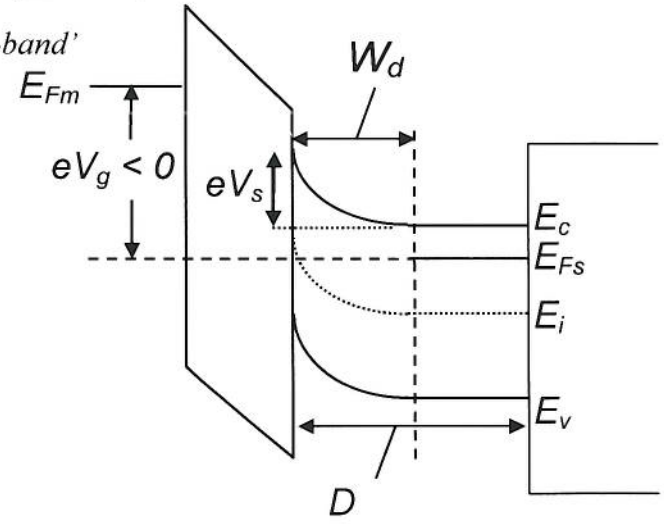

Fig. A3.1b. Depletion

[5]

(b) The charge density $\rho(x)$ vs. x, along the line *AA'*, is shown in Fig. A3.2 below:

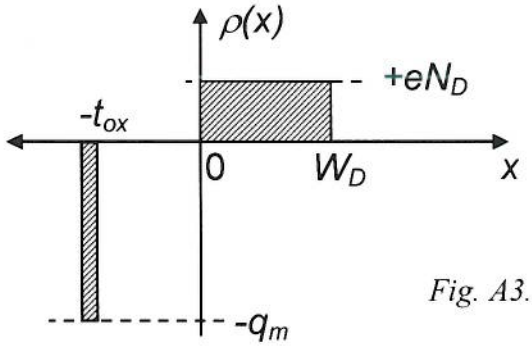

Fig. A3.2

[5]

(c) Poisson's equation, in the Si, is as follows:

$$-\frac{\partial^2 V}{\partial x^2} = \frac{\partial F}{\partial x} = \frac{\rho}{\varepsilon_{Si}\varepsilon_0} = \frac{eN_D}{\varepsilon_{Si}\varepsilon_0}$$

$\therefore$ Solving for electric field F:

$$F = \int \frac{eN_D}{\varepsilon_{Si}\varepsilon_0} dx = \frac{eN_D x}{\varepsilon_{Si}\varepsilon_0} + c$$

Boundary condition $F = 0$ at $x = W_D \Rightarrow$

$$0 = \frac{eN_D W_D}{\varepsilon_{Si}\varepsilon_0} + c \Rightarrow c = -\frac{eN_D W_D}{\varepsilon_{Si}\varepsilon_0}$$

$$\Rightarrow F = -\frac{eN_D W_D}{\varepsilon_{Si}\varepsilon_0}\left(1 - \frac{x}{W_D}\right)$$

Integrating again, for potential $V(x)$:

$$V = -\int F dx = +\int \frac{eN_D W_D}{\varepsilon_{Si}\varepsilon_0}\left(1 - \frac{x}{W_D}\right) dx = \frac{eN_D W_D}{\varepsilon_{Si}\varepsilon_0}\left(x - \frac{x^2}{2W_d}\right) + c$$

Boundary condition $V = 0$ at $x = W_D \Rightarrow$

$$c = -\frac{eN_D W_D^2}{2\varepsilon_{Si}\varepsilon_0}$$

$$\Rightarrow V = -\frac{eN_D W_D^2}{2\varepsilon_{Si}\varepsilon_0}\left(-\frac{2x}{W_D} + \left(\frac{x}{W_D}\right)^2 + 1\right)$$

$$\Rightarrow V = -\frac{eN_D W_D^2}{2\varepsilon_{Si}\varepsilon_0}\left(1 - \frac{x}{W_D}\right)^2$$

$\therefore$ At $x = 0$, the surface potential V_s is:

$$V_s = -\frac{eN_D W_D^2}{2\varepsilon_{Si}\varepsilon_0}$$

[15]

(d) The threshold voltage V_{th} corresponds to the voltage where the Si layer is completely depleted, i.e. $W_D = D$. We then have:

$$V_{th} = V_{ox} + V_s = -\frac{eN_D W_D}{C_{ox}} + V_s$$

Substituting for V_s from part (c), and using $W_D = D$ gives V_{th}:

$$V_{th} = -\frac{eN_D D}{C_{ox}} - \frac{eN_D D^2}{2\varepsilon_{Si}\varepsilon_0}$$

Here, gate capacitance $C_{ox} = \varepsilon_0\varepsilon_{ox}/t_{ox}$.

[5]

Answer, Question 4

a) The four main transduction mechanisms are: electrostatic, magnetic, piezoelectric and piezoresistive.

Electrostatic transduction relies on the variation in capacitance between fixed and moving capacitor plates.

Magnetic transduction may be based either on the variation of inductance caused by movement of parts in a magnetic circuit, or on electromagnetic induction.

Piezoelectric transduction relies on the piezoelectric effect whereby externally applied stress generates dielectric polarisation in a material and hence surface charge which can be measured by a suitable readout circuit.

Piezoresistive transduction relies on the change in electrical resistivity due to externally applied stress.

The most widely used mechanisms are electrostatic and piezoresistive. This is because they can be implemented within a silicon mechanical layer. Magnetic and piezoelectric transduction both require the introduction of other materials. [8]

b) The piezoresistor is aligned to the <100> directions, and the piezoresistive equations (see *Information for Candidates*) are also referred to these directions. We will assume that the (1,2,3) axes are obtained by rotating the (x,y,z) axes by 45° about the z-axis. Then the transverse and longitudinal directions for the piezoresistor will correspond to the 1 and 2 axes respectively.

In this case, the applied voltage V_{BA} will generate a field component $E_2 = V_{BA}/l$, and a current density $J_2 = V_{BA}/(l\rho_e)$. Note that we have neglected the effect of stress on the longitudinal resistance, as instructed.

If there is a shear stress component τ_{12}, the current density J_2 will give rise to a transverse electric field component $E_1 = \rho_e J_2 \pi_{44} \tau_{12} = \pi_{44} \tau_{12} V_{BA}/l$. The potential drop measured across the resistor will then be $V_{CD} = wE_1 = \pi_{44} \tau_{12} V_{BA}(w/l)$ as required. [8]

To relate the shear stress τ_{12} to the axial stresses σ_x and σ_y, we consider the equilibrium of the triangular element below:

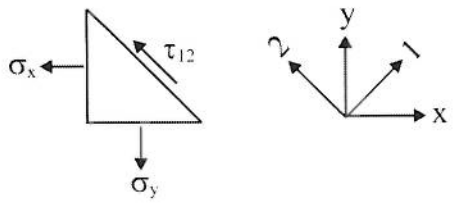

Resolving forces along the 2 direction, taking into account the different side lengths, gives:

$$\sigma_x \cdot 1 \cdot \cos 45° - \sigma_y \cdot 1 \cdot \cos 45° + \tau_{12} \cdot \sqrt{2} = 0$$

$$\Rightarrow \tau_{12} = (\sigma_y - \sigma_x)/2 \qquad [6]$$

Because of the location of the piezoresistor, we know that $\sigma_y = \sigma_{max}$, where σ_{max} is the maximum membrane stress (see *Information for Candidates*), and also that $\sigma_x = \nu\sigma_y$ where ν is Poisson's ratio.

We can therefore write the output voltage as:

$$V_{CD} \approx 0.3\pi_{44}\frac{(1-\nu)}{2}\left(\frac{w}{l}\right)\left(\frac{L}{h}\right)^2 V_{BA} \cdot p$$

Substituting $\pi_{44} = 138.1 \times 10^{-11}$ Pa^{-1}, $\nu = 0.064$, $w/l = 0.2$, $L/h = 1000/20 = 50$, $V_{AB} = 5$ V and $p = 1$ kPa, this gives $V_{CD} = 485$ μV. [8]

Answer, Question 5

a) Applying the method of sections to the flexure in Figure 5.1, the bending moment is found to be:

$$M = P(L-x) - F(v_L - v) - C$$

where $v_L = v(L)$ is the end deflection.

Taking moments for the overall structure gives $PL - Fv_L - 2C = 0$, and this allows us to eliminate the term in v_L giving:

$$M = -Px + Fv + C$$

The elementary bending equation is therefore:

$$EI\frac{d^2v}{dx^2} = -Px + Fv + C \quad \text{or} \quad \frac{d^2v}{dx^2} - \frac{F}{EI}v = \frac{C - Px}{EI}$$

which is the required form. [6]

The general solution is:

$$v = A\cosh(\kappa x) + B\sinh(\kappa x) + \frac{Px - C}{F}$$

The boundary conditions $v = 0$ and $v' = 0$ at $x = 0$ give $A = C/F$ and $B = -P/\kappa F$.

The boundary condition $v' = 0$ at $x = L$ then gives $C = P(\cosh\kappa L - 1)/(\kappa\sinh\kappa L)$.

With these values for A, B and C, the end deflection is given by:

$$v_L = \frac{P}{F}\left[\frac{(\cosh\kappa L - 1)^2}{\kappa\sinh\kappa L} + L - \frac{\sinh\kappa L}{\kappa}\right]$$

and the stiffness is:

$$k = \frac{P}{v_L} = F\frac{\kappa\sinh\kappa L}{(\cosh\kappa L - 1)^2 + \kappa L\sinh\kappa L - \sinh^2\kappa L}$$

which, with the application of the identity $\cosh^2 x - \sinh^2 x = 1$ reduces to:

$$k = \frac{F}{L}\cdot\frac{\kappa L\sinh(\kappa L)}{2[1-\cosh(\kappa L)] + \kappa L\sinh(\kappa L)}$$ [10]

The required approximate form is obtained by replacing the hyperbolic functions with series expansions. Terms up to 6th order need to be considered in the denominator. [4]

b) Assuming the substrate and mass are non-compliant, a temperature rise of ΔT will induce a thermal strain of:

$$\varepsilon = \frac{L_{tot}}{2L}(\alpha_s - \alpha_m)\Delta T$$

where L_{tot} is the total device width (between anchors), L is the length of each flexure, and α_s and α_m are the CTEs of silicon and nickel respectively. This strain will produce an axial load of $F = Ewh\varepsilon$, causing a fractional shift in the stiffness of:

$$\frac{\delta k}{k} \approx \frac{FL^2}{10EI} = \frac{EwhL^2\varepsilon}{10E(w^3h/12)} = \frac{6}{5}\frac{L^2}{w^2}\varepsilon$$

Since the resonant frequency is proportional to √k, the fractional shift in resonant frequency will be:

$$\frac{\delta f}{f} \approx \frac{3}{5}\frac{L^2}{w^2}\varepsilon$$

With L_{tot} = 400 μm, L = 100 μm, w = 5 μm, α_s = 2.5e-6 K^{-1}, α_m = 13.3e-6 K^{-1}, a temperature rise of 1 °C will lead to a strain of $\varepsilon = -2.16 \times 10^{-5}$ and a fractional shift in resonant frequency of $\delta f/f \approx -0.52\%$. [10]